

Electrostatic Interactions between the CTX Phage Minor Coat Protein and the Bacterial Host Receptor
TolA Drives the Pathogenic Conversion of *Vibrio cholerae*.

Laetitia Houot, Romain Navarro, Matthieu Nouailler, Denis Duché, Françoise Guerlesquin and
Roland Llobes

From Laboratoire d'Ingénierie des Systèmes Macromoléculaires, UMR7255, Institut de Microbiologie de
la Méditerranée, Aix-Marseille Univ - CNRS, 31 Chemin Joseph Aiguier, 13402 Marseille Cedex 20,
France

Running title: *Oxi-BTH study of the pIII^{CTX}-TolA binding determinants*

To whom correspondence should be addressed: Dr. L. Houot, Laboratoire d'Ingénierie des Systèmes
Macromoléculaires, UMR7255, Institut de Microbiologie de la Méditerranée, Aix-Marseille Univ -
CNRS, 31 Chemin Joseph Aiguier, 13402 Marseille Cedex 20, France; Tel: +33 491-164-663; Fax: +33
491 712 124; ORCID: 0000-0002-5556-9603; E-mail: lhout@imm.cnrs.fr

Keywords: *Vibrio cholerae*, bacteriophage, protein-protein interaction, protein complex, molecular
motor, bacterial pathogenesis.

ABSTRACT

Vibrio cholerae is a natural inhabitant of aquatic environments and converts to a pathogen upon infection by a filamentous phage, CTXΦ, that transmits the cholera toxin encoding genes. This toxigenic conversion of *V. cholerae* has evident implication in both genome plasticity and epidemic risk, but the early stages of the infection have not been thoroughly studied. CTXΦ transit across the bacterial periplasm requires binding between the minor coat protein named pIII and a bacterial inner-membrane receptor, TolA, which is part of the conserved Tol-Pal molecular motor. To gain insight into the TolA-pIII complex, we developed a bacterial two-hybrid approach, named Oxi-BTH, suited for studying the interactions between disulfide bond-folded proteins in the bacterial cytoplasm of an *E. coli* reporter strain. We found that two of the four disulfide bonds of pIII are required for its interaction with TolA. By combining Oxi-BTH assays, NMR, and genetic studies, we also demonstrate that two intermolecular salt bridges between TolA and pIII provide the driving forces of the complex interaction. Moreover, we show that TolA residue R325 involved in one of the two salt bridges is critical for proper functioning of the Tol-Pal system. Our results imply that to prevent host evasion, CTXΦ uses an infection strategy that

targets a highly conserved protein of Gram-negative bacteria essential for the fitness of *V. cholerae* in its natural environment.

Phage-bacterium interaction is one of the driven forces for gene acquisition and bacterial host adaptation to their environment, and has been frequently associated with increased virulence of the bacterial host. A striking example of this parasitism-dependent adaptation is *Vibrio cholerae*, a bacterial natural inhabitant of estuarine, and the causative agent of epidemic disease cholera. While there are more than 200 O-antigen serogroups described, only two have been reported to cause the pandemic disease cholera: the O1 and O139 serotypes, due to the production of two essential virulence factors: the Toxin Co-regulated Pilus (TCP) and the Cholera Toxin (CT). Interestingly, the genes *ctxAB* encoding the enterotoxin CT are not carried by the core genome of the bacterium, but can be acquired after infection by a lysogenic bacteriophage known as CTXΦ (1). Once infected, the bacterium produces CT, and assembles new phage particles (carrying the *ctxAB* genes) that will be secreted in the environment, and may convert non-pathogenic *V. cholerae* cells to pathogenicity.

Most of the knowledge on CTX Φ infection have been extrapolated from the canonical model of *Escherichia coli* F-pilus-specific coliphages Ff (including f1 Φ , fd Φ , and M13 Φ). CTX Φ and Ff Φ both belong to the genus *Inovirus* that are filamentous particles containing a circular single-stranded DNA genome. The genome of inoviruses comprises about ten genes and is generally organized in a conserved modular structure in which functionally related genes are grouped together (For review, see (2, 3)). Ff Φ and CTX Φ binding and uptake into the host cell relies primary on the minor coat protein pIII located at the distal tip of the phage, and present at three to five copies. While there is no sequence conservation between pIII^{Ff} and pIII^{CTX}, both proteins are composed of three distinct domains separated by two Low-Complexity Regions (LCR) that serve as linkers. While the N-terminal (N1) and the central domains (N2) are exposed at the capsid surface, the C-terminal domain (N3) anchors the pIII protein to the phage particle through hydrophobic interactions (4–6).

Filamentous phage infection of the bacterial host is seen as a sequential two-step process. First, phage recruitment occurs upon specific binding between the phage capsid pIII-N2 domain and a primary receptor exposed at the surface of the cell host: the conjugative F pilus for *E. coli* (3, 7) and the Toxin Co-regulated Pilus TCP for *V. cholerae* (1, 5). In *E. coli*, ATP-dependent retraction of the F pilus brings the phage in contact with the cell envelope, promoting its transport across the outer membrane (OM) by an unknown mechanism. Then, pIII must partially unfold to separate N1 and N2 domains (8). This event is crucial in the infection process as it unmasks pIII-N1 domain for subsequent binding to a second receptor: the TolA^{Ec} protein located in the cell envelope (8–12). In *E. coli*, it has been proposed that the pIII-N1^{Ff}/TolAIII^{Ec} interaction triggers conformational modifications permitting the pIII-N3 domain to form a pore in the bacterial IM, allowing the subsequent phage DNA injection into the cell cytoplasm (13). The nature of the force driving the DNA out of the capsid remains unknown.

In *V. cholerae*, TCP retraction seems central to the phage infection process, as TCP production alone is not sufficient to allow CTX Φ uptake (14). While TCP parasitism facilitates the introduction of CTX Φ into the host cell, subsequent phage binding to TolA^{Vc} appears to be the limiting step

of the infection process (5, 6, 15). Thus, Waldor and collaborators have shown that a chimeric fd phage displaying the pIII-N1^{CTX} domain fused to the pIII-N3^{fd} domain can successfully infect *V. cholerae* cells. This demonstrates that the pIII-N1^{CTX} domain displayed at the tip of the capsid is critical and sufficient to assure host specific recognition in a TCP-independent manner (5).

TolA is the central protein of the Tol-Pal cell envelope system, which is highly conserved in Gram-negative bacteria (16, 17). In addition to TolA, the Tol-Pal complex is composed of two IM proteins, TolQ and TolR, of the outer membrane (OM) lipoprotein Pal and of the periplasmic protein TolB. In several species, including *E. coli* and *V. cholerae*, two additional proteins complete the system: the periplasmic protein CpoB (previously YbgF) (18) and the cytoplasmic thioesterase YbgC (19). The Tol-Pal complex is suspected to function as a nanomachine, using the proton-motive force (pmf) of the IM to generate movements and to transfer energy to OM proteins. Multiple interactions connecting the different components of the Tol-Pal system have been identified. TolA, TolQ and TolR form a complex anchored in the IM. The TolA protein extends in the periplasm thanks to a long α 2-helix (TolAII domain) while its globular C-terminal domain (TolAIII) interacts with TolB, and with Pal in the presence of pmf (20–22). Moreover, Pal interacts with TolB and with the peptidoglycan (PG) (23). Thus, the Tol-Pal system links the IM, the OM and the PG. The system is involved in maintaining OM integrity, conferring pleiotropic phenotypes when one of its genes, is mutated: increased sensitivity to detergents, cell filamentation in low and high osmolarity media, and outer membrane hypervesiculation (6, 24). In addition, the Tol system is involved in the late stage of cell division corresponding to the OM constriction (25) and has been found associated with the PBP1B-LpoB complex in *E. coli* (18). It is also required for proper localization of polar factor in *Caulobacter crescentus* (26) and of chemoreceptors in *E. coli* (27).

For both coliphage and CTX Φ , structural studies on isolated protein domains have provided new insights into the complex formed with TolAIII in the bacterial periplasm (Fig. 1). First, the structures demonstrate that although the CTX Φ pIII-N1 and M13 Φ pIII-N1 domains have only 15% sequence identity, they are both dominantly

composed of β -strands, and multiple disulfide bonds stabilize their structures. On the bacterial side, TolAIII^{Ec} and TolAIII^{Vc} are curved structures mixing α -helices and β -sheets. A high-resolution structure of *E. coli* TolAIII free in solution has been obtained by heteronuclear NMR (Protein Data Bank PDB #1S62) (12), while TolAIII in complex with coliphage pIII-N1^{M13} (residues 11 to 86) has been obtained by X-ray crystallography (PDB #1Tol). The structure shows that pIII-N1^{M13} domain binds the concave side of TolAIII^{Ec}, forming a continuous interprotein β -sheet (8). In 2012, Ford and collaborators determined the crystal structure of pIII-N1^{CTX} domain alone and in complex with *V. cholerae* TolAIII domain (PDB #4G7X). Surprisingly, the authors showed that pIII-N1^{CTX} binds on the convex face of TolAIII^{Vc}, resulting in a continuous interprotein β -sheet (Fig. 1A). Thus, interaction between the two partners delineates a distinct interface compared to the coliphage model of infection (15).

Filamentous phages are not the only particles that parasitize the Tol-Pal system to penetrate *E. coli* cells. Colicins are bacterial toxins comprising various types of lethal activity targeting the IM, the RNA, or the peptidoglycan of its bacterial target. Tol-dependent colicins have been shown to interact with one or more of the Tol proteins during their translocation across the periplasm, showing some similarities with Tol-dependent filamentous phage uptake. In 2012, Li and collaborators demonstrated that a Colicin A peptide (residues 53 to 107) binds on the convex face of TolAIII^{Ec}, forming an intermolecular antiparallel β -sheet (28).

It is puzzling to observe that despite the structural similarities between *V. cholerae* and *E. coli* TolAIII domains, the molecular binding interfaces with colicin A, pIII^{CTX} and pIII^{M13} differ, illustrating the versatile functioning of TolA as a periplasmic hub protein. In the present study our goal was to investigate the determinants allowing CTX Φ specific host selection and periplasm transit *in vivo* thanks to a new oxidative bacterial two-hybrid approach combined to NMR and *in vivo* studies.

Results

Development of an oxidative bacterial two-hybrid approach dedicated to disulfide bond folded

protein analysis— To gain insights into the mechanism of CTX Φ transit through the periplasm, we first analyzed the interaction that occurs between pIII-N1^{CTX} and TolAIII^{Vc}, compared to the pIII-N1^{M13} and TolAIII^{Ec} interaction, using a bacterial two-hybrid (BACTH) approach. This system relies on the reconstitution of the signaling cAMP transduction cascade in an endogenous adenylate-cyclase-deficient strain (29). The TolAIII domains from *V. cholerae* and from *E. coli* were fused to the T18 domain in the pUT18 vector, while the pIII-N1 domain from M13 and CTX phages were fused to the T25 domain in the pKT25 vector. Constructs were introduced into the *E. coli* BTH101 strain and co-transformants were tested on MacConkey plates. As a control, we first observed that in this assay, the T18-TolAIII^{Ec} construct gives a positive interaction signal with the colicin A N-terminal domain (ColA^N) as previously described (10, 22, 30), which validated our approach (Fig. 1B, left panel). We also observed that a T18-TolAIII^{Vc} construct is unable to bind T25-ColA^N, attesting the specificity for partner recognition between the two bacterial species. Then, we tested the TolAIII^{Vc} and pIII-N1^{CTX} constructs together, but we did not detect interaction between these different domains. We obtained the same negative result when we tried to detect TolAIII^{Ec}/pIII-N1^{M13} interaction (Fig. 1B, left panel). We hypothesized that this result could arise from improper folding of disulfide-bonded TolAIII, pIII-N1^{M13} or pIII-N1^{CTX} domains when expressed in the cell cytoplasm (Fig. 2, A and B).

Thus, we envisioned that a bacterial two-hybrid assay in an oxidative environment would allow the proper folding of proteins with disulfide bonds. Several *E. coli* strains, such as Origami (Novagen) or SHuffle (New England Biolabs) have been engineered to optimize the purification of proteins with disulfide bonds and are commercially available. We chose the SHuffle T7 strain as a chassis because it is deleted for glutaredoxin reductase (*gor*) and thioredoxin reductase (*trxB*) genes, allowing disulfide bond formation in the cytoplasm. In addition, this strain expresses a cytoplasmic version of the disulfide bond isomerase DsbC, promoting correct disulfide bond formation and proper oxidative folding of proteins containing multiple cysteines (31). We transduced the *cya* mutation in the SHuffle strain to make the Oxi-BTH strain (for Oxidative

Bacterial Two-Hybrid). The resulting strain was co-transformed with the pUT18 and pKT25 vectors expressing domains of interest. As shown on Figure 1B (right panel), the Oxi-BTH strain allowed the detection of interaction between TolAIII^{Vc} and pIII-N1^{CTX}, as well as between TolAIII^{Ec} and pIII-N1^{M13}. Thus, we concluded that the Oxi-BTH strain is a powerful tool to apply the BACTH system to the study of disulfide-bonded proteins. Indeed, our data suggest that in both *E. coli* and *V. cholerae*, disulfide bond-dependent folding of the TolAIII domain and/or the phage minor capsid domain is required to allow binding of the two partners. Conversely, TolAIII^{Ec} is able to interact with the colicin A N-terminal domain, that does not contain cysteines, in both reducing and oxidizing conditions (Fig. 1B). Finally, we did not observe cross-interaction between the two species (i.e. TolAIII^{Vc}/pIII-N1^{M13} or TolAIII^{Ec}/pIII-N1^{CTX}) despite strong structural conservation between *E. coli* and *V. cholerae* TolAIII domains.

Role of disulfide bonds in TolAIII^{Vc}/pIII-N1^{CTX} interaction— Because TolAIII^{Vc}/pIII-N1^{CTX} interaction is only seen in our oxidative two-hybrid assay, we hypothesized that one or more disulfide bonds might be essential for bacterial and phage domain recognition. To test this hypothesis, each disulfide bond (one in TolAIII^{Vc} and four in pIII-N1^{CTX}, Fig. 2, A and B) was sequentially abolished by introducing substitutions of individual cysteine to serine in the BACTH constructs. The resulting mutants were then tested in the Oxi-BTH assay. As shown on Figure 2C, TolAIII^{Vc} (C292S) construct was still able to interact with pIII-N1^{CTX}. This suggests that disulfide bond formation in TolAIII^{Vc} is not required for CTX phage binding. We then targeted each of the four disulfide bonds present in pIII-N1^{CTX}. None of the individual mutations we performed was able to totally abolish binding to TolAIII^{Vc}. Interestingly, mutation of the second or the third S-S bond (mutations C47S and C75S, respectively) of the phage pIII-N1 domain resulted in a faint interaction signal, suggesting a weaker binding affinity between TolAIII^{Vc} and these two pIII-N1^{CTX} mutants compared to the wild-type construct. In agreement with this observation, a pIII-N1^{CTX}(C47S-C75S) double mutant was not able to interact with TolAIII^{Vc}. These observations are unlikely to result from stability defects of the

cysteine variants compared to the native pIII-N1 protein. Indeed, inserting the same mutations on the his-tagged pIII-N1^{CTX} domain expressed from the pIN vector resulted in equivalent expression of the different constructs (Fig. S1). Moreover, as the pIII-N1^{CTX}/TolAIII interaction is not seen in the regular BACTH assay, it is more likely that pIII-N1^{CTX} folding *via* its 2nd and 3rd disulfide bonds is critical for TolAIII^{Vc} binding.

The CTXΦ central domain pIII-N2 does not block phage pIII-N1 accessibility to TolAIII^{Vc}— It has been shown that Ff coliphages require an activation step to become able to infect the host cell. Indeed, in the native conformation of the minor capsid protein pIII^{Ff}, the N2 domain is tightly associated to N1, which buries the phage TolAIII-binding site at the domain interface. Phage activation is processed upon binding of N2 to the primary receptor, the F pilus, which initiates partial unfolding, prolyl cis-to-trans isomerization in the hinge between N1 and N2 and domain disassembly, thereby exposing its binding site for the ultimate receptor TolA (32). It has been proposed that the isomerization sets a molecular timer to maintain the binding-active state long enough for the phage to interact with TolA. Conversely, Craig and collaborators have suggested that the TolA binding site on pIII-N1^{CTX} is permanently accessible and does not require initial pilus-induced conformational change (15). We wondered if a fusion to the two-hybrid T25 domain would allow us to test the influence of pIII-N2^{CTX} on the accessibility of pIII-N1^{CTX} in an Oxi-BTH interaction assay. Indeed, our data show that the T25-pIII-N1N2^{CTX} construct is able to bind T18-TolAIII^{Vc}, while the T25-pIII-N2^{CTX} domain alone is not (Fig. 2C). This result demonstrates that pIII-N1^{CTX} exposes a TolAIII^{Vc} binding motif that is not masked by the pIII-N2 domain.

Specific recognition between the TolAIII^{Vc} and pIII-N1^{CTX} domains relies on two salt bridges— We aimed to identify the residues showing a predominant role in the specificity of binding. Reversible protein-protein interactions involve low energy ionic bonds, hydrogen bonds and van der Waals interactions. Based on the co-crystal structure of TolAIII^{Vc} and pIII-N1^{CTX} (PDB #4G7X; (15)) we focused our analysis on the intermolecular salts bridges. Residues K324, R325

and K347 on TolAIII^{Vc} respectively interact with E37, D39 and E92 on pIII-N1^{CTX} (Fig. 3A). In order to analyze the importance of these three salt bridges in the complex formation, we abolished them sequentially by introducing single residue substitutions on TolAIII^{Vc}. We confirmed that the different TolAIII^{Vc} variants showed production level and stability equivalent to the wild-type T18-TolAIII construct by immunodetection (Fig. 3B), and tested their capacity to interact with T25-pIII-N1 in a Oxi-BTH assay (Fig. 3C). The TolAIII(K324E) and TolAIII(R325D) mutants were respectively partially, and totally impaired in their ability to interact with pIII-N1^{CTX}, while the TolAIII(K347E) mutant retained its ability to bind pIII-N1^{CTX}. Conversely, we introduced the mirror mutations on T25-pIII-N1^{CTX} to generate the E37Q-D39N and the E92K variants. We demonstrated that T25-pIII-N1(E37Q-D39N) was unable to bind T18-TolAIII^{Vc}, while T25-pIII-N1(E92K) was. Together, these data suggested that the two intermolecular salt-bridges engaged between K324 and R325 on TolAIII^{Vc}, and E37 and D39 on pIII-N1^{CTX} are crucial for pIII-N1/TolAIII^{Vc} complex stabilization.

To confirm the role of the TolAIII charged patch [K324-R325] in pIII-N1^{CTX} binding, we swapped the charged residues engaged into salt-bridges between the two partners. As predicted, the T18-TolAIII(K324E-R325D) double mutant was not able to interact with the wild-type T25-pIII-N1^{CTX} construct but regained interaction with the mutated variant presenting opposite charged residues T25-pIII-N1(E37K-D39R) (Fig. 3C). Of note, the restored interaction signal appeared weaker than the one observed for wild-type constructs, possibly reflecting that additional local steric effects operate at the binding interface.

To further establish that our data result from a specificity of interaction rather than a folding defect of the protein variants, we developed a NMR approach. We used the pIN3-ompA2 vector (33) to overproduce ¹⁵N-labelled wild-type pIII-N1^{CTX}, pIII-N1^{CTX}(E37Q-D39N) and pIII-N1^{CTX}(E92K) variants fused to a His C-terminal tag. The ¹H-¹⁵N HSQC spectra of the proteins (Fig. 4A, 4C and 4E) shows ¹⁵N/¹H correlations for the NH group of each amino acid of the proteins. The ¹⁵N and ¹H resonances are associated to the nucleus chemical environment, thus ¹H-¹⁵N HSQC spectrum represents the finger print of a protein. In the case of the native and variant pIII-N1^{CTX}, the

¹H-¹⁵N HSQC spectra are well resolved. This indicates that each residue has a particular environment in agreement with the x-ray structure of the protein (15). The fact that the spectra of the variant proteins are similar to that of the native protein demonstrates the conservation of the folding. Moreover, superimposition ¹H-¹⁵N HSQC in the presence and the absence of TolAIII^{Vc} showed chemical shift perturbations for pIII-N1^{CTX} (Fig. 4B) and pIII-N1^{CTX}(E92K) variant (Fig. 4D), while no perturbation was seen with the pIII-N1^{CTX}(E37Q-D39N) variant (Fig. 4F). These observations demonstrate that pIII-N1^{CTX} and pIII-N1^{CTX}(E92K) could interact with the TolAIII^{Vc} domain, modifying the chemical environment of nucleus located at the interface, while the pIII-N1^{CTX}(E37Q-D39N) variant could not, which confirmed the Oxi-BTH results.

In V. cholerae, periplasmic expression of the CTX pIII-N1 domain leads to tol phenotypes— Oxi-BTH assay and NMR studies allowed us to identify key residues on the CTXΦ minor capsid protein that were involved in TolAIII binding. In order to confirm these data *in vivo*, we used a periplasmic expression assay in *V. cholerae*. In *E. coli*, it has been previously shown that production of the N-terminal domain of colicin A (34) or of pIII-N1 domain of coliphage f1 (10) into the periplasm of WT cells perturbs the Tol-Pal system by sequestering the TolA protein, and consequently results in *tol* phenotypes. This approach is particularly suitable to study the translocation step of phage infection, as it does not require production and assembly of mutated phage particles, their TCP-dependent reception and their OM transport.

We used the pIN3-ompA2 vector to express the his-tagged pIII-N1^{CTX} wild-type sequence (or variants) fused to a N-terminal *ompA* signal sequence in order to allow transport of the produced proteins into the periplasm via the *sec* pathway. Correct production of the resulting proteins in *V. cholerae* cells was confirmed by immunodetection, while transport of the produced domains into the periplasm was attested by sodium azide inhibition of the *sec* pathway (Fig. S2). Cells producing the WT pIII-N1 phage domain targeted to the periplasm presented a 5-fold decrease in susceptibility to phage infection (Fig. 5A), high sensitivity to deoxycholate (DOC) (Fig. 5B) and to sodium dodecyl sulfate (SDS) (Fig. 5C), which are

characteristic *tol* phenotypes. This suggests that the exogenous pIII-N1^{CTX} domain interacts with the endogenous TolA^{Vc} protein in *V. cholerae* cell envelope, competing with the other Tol proteins of the system, and preventing adequate functioning that insures membrane integrity and permits phage uptake. We also observed that exogenous production of pIII-N1^{M13} in *V. cholerae* periplasm does not result in *tol* phenotypes, which demonstrates further that the M13Φ capsid protein pIII does not bind *V. cholerae* TolA protein. In accordance with the Oxi-BTH results, periplasmic expression of the pIII-N1^{CTX}(E37Q-D39N) construct resulted in phage infection rate, DOC sensitivity and SDS sensitivity similar to the control cells carrying an empty vector, while periplasmic expression of the pIII-N1^{CTX}(E92K) variant showed the same phenotypes as those obtained with the WT pIII-N1^{CTX} construct. In accordance with the Oxi-BTH results, these *in vivo* data confirm that the pIII-N1^{CTX} negatively charged residues E37 and D39 are required for pIII-N1 interaction with the native TolA protein.

Evidence that TolA R325 residue is essential to the Tol-Pal system proper functioning in V. cholerae— We decided to investigate if the TolA charged patch [K324-R325] required for phage binding is important for the Tol-Pal system function in *V. cholerae*. While multiple attempts to delete *V. cholerae* full length *tolA* gene by double homologous recombination were unsuccessful, we found that a TolAΔ(41-421) mutant, deleted for its periplasmic domains but retaining its IM domain, is viable. The resulting strain presents characteristic *tol* phenotypes (6, 35), including resistance to CTXΦ infection, sensitivity to SDS and to DOC, and finally growth defect in a low osmolarity medium (tryptone broth, 66 mM NaCl) compared to LB medium (Fig. 6, A-E).

We first performed a complementation assay of the TolAΔ(41-421) mutant using a pBAD expression vector. TolA has been reported to be a low abundance protein (400 to 800 copies in *E. coli* cells, (36)). In our assay, basal level of TolA production from the pBAD-TolA vector was detected even in the absence of induction (Fig. 6A), and was sufficient to almost fully complement (80% to 100% rescue) the *V. cholerae* *tolA* mutant for phage infection (Fig. 6B), for resistance to SDS and DOC (Fig. 6C and 6D) and for hypo-osmotic growth in tryptone broth (Fig.

6E). These results also confirmed that the deletion had no polar effect on the other genes of the Tol-Pal operon.

We then tested *V. cholerae* strains carrying TolA variants where residues K324, R325 or K347 were mutated for opposite charged residues. While the K324E variant behaved similarly to the wild-type pBAD-TolA construct, rescue was no longer observed for the TolA(R325D) variant, in spite of adequate production of the mutant protein (Fig. 6A-E). The TolA(K324E-R325D) double mutant showed a slightly stronger phenotype than the individual mutants for membrane integrity assays (Fig. 6C and 6D). Finally, the TolA(K347E) variant complemented the mutant strain similarly to the WT TolA construct. Together, these findings support the conclusion that the positively charged residue R325 plays a dominant role in TolA function in *V. cholerae*, while K324 and K347 do not.

Conservation of the K324 and R325 residues in other TolA Vibrio species— The Tol-Pal system has a widespread distribution in Gram-negative bacteria. We first questioned TolA sequence conservation among 128 *Vibrio cholerae* isolate genomes available on NCBI database, and found that the full-length protein is 100% identical (Fig. S3). We then broaden the study to the vibronaceae family, including 82 *Vibrio* species (Fig. S4) and 33 non-*Vibrio* species (6 *Aliivibrio*, 3 *Enterovibrio*, 5 *Grimontia*, 13 *Photobacterium* and 6 *Salinivibrio*; Fig. S5). PSIPRED analysis (37) of the TolAIII amino acid sequences suggests that the secondary structures are conserved among Vibrionaceae (data not shown). Alignments of TolAIII sequences from multiple *Vibrio* species indicates that K324 is highly conserved (73/82 sequences) with only few variants where it is replaced by another positively charged residue, arginine (6/82). Three exceptions were found with *V. breoganii*, *V. gazogenes* and *V. rhizosphaerae* that carry an uncharged glutamine residue at position 324. Overall, the positive charge at position 324 appears to be conserved in other Vibrionaceae tested (31/33), suggesting its importance in TolA function (Fig. S4 and S5). Conversely, the positively charged residue R325 is less conserved in *Vibrio* species (51/82), frequently being replaced by the uncharged residue serine (25/82) or less frequently by alanine, threonine or valine (6/82). Notably, the

positively charged residue at position 325 was never observed in other Vibrionaceae species (0/33).

As we previously demonstrated that pIII-N1^{CTX} interaction with the *V. cholerae* TolA receptor is driven by two intermolecular salt-bridges engaging TolA K324 and R325 residues, we expected orthologous TolAIII sequences carrying the charged patch [K324-R325] to also be able to bind CTX pIII-N1. As shown in Figure 7A, the TolAIII domain from *V. anguillarum*, *V. tasmaniensis* and *V. alginolyticus* carry the [KR] patch, while *V. harveyi* has a [KS] motif and the Vibrionaceae *Aliivibrio fischeri* has a [KT] motif. The TolAIII coding sequences from the different species were cloned into the pUT18 vector and correct expression of the different constructs was assessed by immunodetection (Fig. 7B) before testing their interaction ability with T25-pIII-N1^{CTX} in the Oxi-BTH assay. As shown on Figure 7C, T18-TolAIII from *V. anguillarum*, *V. tasmaniensis* and *V. alginolyticus* showed positive interaction signal with T25-pIII-N1^{CTX}. In contrast, T18-TolAIII^{*V.harveyi*} and T18-TolAIII^{*V.fischeri*}, lacking the positively charged patch [KR], were not able to bind pIII-N1^{CTX}. We analyzed the TolAIII sequences that were able to bind pIII-N1 in order to define a consensus sequence for partner recognition. We found that TolAIII tolerates multiple sequence variation in the β 2-strand, likely because this region of the protein interacts with pIII-N1 β 1-strand through backbone hydrogen-bond interactions. Conversely, TolAIII α 2-helix alignments allowed the definition of a consensus sequence

[GD(S/T)R(L/V)CAA(T/A)KRA(V/I)AQ]

surrounding the [KR] residues. We noticed that *V. harveyi* TolAIII carry the defined consensus sequence, apart from R325. However, point mutation to generate T18-TolAIII^{*V.harveyi*} S325R and reconstitute a positively charged patch [KR] was not sufficient to restore interaction with pIII-N1^{CTX} (Fig. 7C).

Discussion

A new in-vivo protein-protein interaction assay dedicated to disulfide oxidized proteins— For many proteins functioning in the periplasm, exposed at the cell surface, or secreted in the extracellular environment, stability and/or activity

require the formation of disulfide bonds. For example, in *V. cholerae*, S-S bonds proteins include the cholera toxin (38), the pilin subunits that assemble in different type IV pili (TCP, MshA, PilA) operating into the various aspects of *Vibrio* ecology (39, 40), the TolA protein in the Tol-Pal complex involved in envelope integrity and cell division (15) and sensors such as TcpP (41, 42) and ToxR (43) operating signal transduction to regulate virulence pathways. Thus, identification and characterization of physiologically relevant interactions between these S-S bond proteins *in vivo* is a crucial task for the understanding of molecular processes within the cell.

The original BACTH approach is an easy yet efficient technic that has become a common laboratory tool used to identify and dissect protein-protein interactions (29, 44). As the interaction between candidates of interest is tested in the cell cytoplasm, studies were restricted so far to proteins in their reduced state. Recently, the development of new BACTH plasmids inserting a transmembrane segment downstream of the T25 and T18 fragments was shown to allow the detection of interactions occurring within the periplasmic space of the cell (45).

In this study, we extended the range of BACTH application to the study of disulfide-oxidized proteins directly in the reporter cell cytoplasm thanks to a new genetic background, that we named Oxi-BTH. In this strain, correct disulfide reshuffling is catalyzed by a cytoplasmic version of the disulfide bond isomerase DsbC (31). The Oxi-BTH assay was validated by the visualization of interactions previously described between proteins with unique (TolAIII^{Ec}, TolAIII^{Vc}) and multiple disulfide bonds (pIII-N1^{M13}, pIII-N1^{CTX}), that could not be observed in the regular BACTH assay. As a protein with 8 cysteines, pIII-N1^{CTX} has a probability of less than 1% to form the correct four disulfide bonds, our results also attest the efficiency of the cytoplasmic DsbC proofreading activity (Fig. 1). Finally, this tool was suitable to individually test the importance of each disulfide bond and of targeted residues in protein-protein interactions (Fig. 2 and 3). Many BACTH pUT18 and pKT25 constructs have already been published, and genome-wide libraries are available for *E. coli* (46) and *P. aeruginosa* (47) allowing the constitution of a large collection of potential partners that can be directly tested in

the Oxi-BTH assay without requiring new cloning steps. In this context, we believe that Oxi-BTH constitutes a robust and versatile tool to test the importance of oxidative folding in protein-protein interaction, to identify key amino acids involved, and to investigate the specificity of binding between two proteins of interest.

Refining the model of CTXΦ uptake— Filamentous phage infection is a two-steps process, requiring a primary receptor at the surface of the cell (the TCP pilus in the case of CTXΦ) and a secondary receptor, TolA, inside the cell envelope. In this study, our aim was to gain insight into the second step of the infection process by investigating *in vivo* the phage-TolA interaction. At the contrary to *E. coli*, we did not manage to obtain the *V. cholerae* TolA clean deletion mutant by homologous recombination, while we were able to delete the periplasmic domains of the protein. It is worthy to note that the only other *V. cholerae* TolA⁻ mutant published in the literature is a *tolA::pGP704* disruption mutant (obtained by single crossover) that, according to the primer design, also resulted in a truncated TolA protein somewhere in the periplasmic domain (6). This suggest that, in laboratory conditions, TolA is essential in *V. cholerae*, as previously reported in *E. coli* O7:K1 (48), *Pseudomonas aeruginosa* (49) and *Caulobacter crescentus* (26), while being dispensable *E. coli* K12 strain (35).

We observed that pIII-N1^{CTX} domain is sufficient for TolA binding, and that pIII-N2^{CTX} doesn't impede the interaction between the two partners (Fig. 2). This result is in agreement with previous observations made by Ford and collaborators (15). Indeed, the authors previously showed that CTXΦ incubation with an excess of purified TolAIII^{Vc} domain before infection of *V. cholerae* O395 cells reduced the infection efficiency. However, in this study, binding between pIII-N1-N2^{CTX} and TolAIII^{Vc} had not been formally tested because pIII-N1-N2^{CTX} could not be purified in a soluble form (15). Together, our data further demonstrate that the CTXΦ naturally exposes a TolA-binding site on the N-terminal domain of pIII, which is reminiscent to IF1 and IKe coliphage infection strategy (50). It implies that CTXΦ binding to the primary receptor TCP might be responsible for phage recruitment from the environment and possibly active pulling to the cell surface through retraction (14) but is not required to unmask pIII-N1 TolA binding site.

The crystal structure of the complex (PDB #4G7X) suggested that multiple interactions (ionic, hydrophobic, polar contacts and van der Waals forces) contribute to the binding interface between TolAIII^{Vc} and pIII-N1^{CTX}. The TolAIII^{Vc} β2-strand folds around pIII-N1^{CTX}, resulting in a continuous intermolecular β-sheet that involves multiple hydrogen bonds between the backbone chains of TolAIII β2-strand and pIII-N1 β1-strand. TolAIII^{Vc} residues K324, R325 and K347 form three salt bridges with pIII-N1 E37, D39 and E92 residues, respectively (Figure 3). However, the contribution of each of the individual interaction in the TolAIII/pIII^{CTX} complex formation cannot be assessed from the crystal structure. By combining *in silico* analysis and *in vivo* experimental data, we defined that the consensus sequence for CTX binding on TolAIII^{Vc} is restricted to the α2-helix, while the β2-strand tolerates multiple residues variations (Fig. 7). Moreover, our work clearly demonstrates that the two salt bridges engaged between TolAIII^{Vc} residues K324 and R325, and CTX phage pIII-N1 residues E37 and D39 respectively, provide the driving forces of the interaction, forming ion locks required for the complex to form, while the TolAIII K347-pIII-N1 E92 bond is dispensable. It is worthy to note that mutating the TolAIII R325 residue alone had a stronger negative impact on phage binding than mutating the TolAIII K324 residue (Fig. 3). We used the 2P2I database (http://2p2idb.cnrs-mrs.fr/2p2i_inspector.html; (51, 52)) in order to gain insights into the protein-protein interface parameters. Results showed a total of 88 non-bonded contacts (distance cutoff 4 Å) between pIII-N1^{CTX} and TolAIII^{Vc} (Fig. S4). Among these 88 contacts, TolAIII R325 was engaged in 20 different contacts with pIII-N1 surface, while TolAIII K324 was engaged in 6. These observations might explain the more predominant role of TolAIII R325 residue in pIII-N1 binding, compared to K324. Overall, this is reminiscent of what was previously observed for M13 coliphage pIII-N1 binding on the concave side of TolAIII^{Ec}, where the interaction makes an antiparallel continuous β-sheet stabilized by two salt bridges (TolAIII^{Ec} D210, K212 interacting with pIII-N1^{M13} R29 and D28, respectively (PDB #1Tol; (8)). It would be interesting to test the importance of each of these ionic interactions for coliphage-TolA^{Ec} complex formation.

TolA is involved in the fitness of *V. cholerae*, in particular in low osmolarity conditions such as those found when the bacterium reach low salinity environments (fresh water), or in response to detergent components, such as the bile acid deoxycholate during its transit through the gastrointestinal track (Fig. 5 and Fig. 6, (6)). We found that the TolA(R325D) variant was functionally unable to complement *V. cholerae* tol mutant, while the TolA(K324E) mutant was (Fig. 6). We questioned the sequence conservation of TolAIII in other vibrio species, but we didn't observe strict correlation between conservation of the K324 and R325 residues and their importance in TolA function in the tested conditions. Interestingly, we noticed that in the 33 Vibrionaceae species studied, the TolAIII R325 residue is absent (Fig. S3), while additional positive charges are found at more or less one pitch of the $\alpha 2$ helix: R321 (occurrence 33/33) and K329 (occurrence 24/33). Because TolA is a hub protein, and part of a multicomponent complex, the patch of positive residues on the $\alpha 2$ helix might be involved in partners binding, either with an already known partner of the TolAIII domain such as TolB or Pal (16, 22, 53) or an unknown partner that still has to be identify.

We demonstrated that the KR patch on TolA is crucial but not sufficient for CTX binding (Fig. 7). Indeed, study of the *V. harveyi* TolA(S325R) variant suggests that additional local steric effects operate at the binding interface, outside the $\alpha 2$ helix. While salt bridges provide the forces to drive protein-protein initial attraction, subsequent complex stabilization is usually the result of cooperative interactions that encompass multiple pairwise bonds (54). Our results allow a better understanding of the TolAIII/pIII-N1 interaction interface, with two salt-bridges providing the driving forces of the interaction while the formation of the intermolecular anticontinuous β -sheet provides stabilization interactions to the complex. By targeting important functional and/or conserved residues of TolA protein, CTX Φ uses a parasite infection strategy that may help to prevent *V. cholerae* from escaping the infection.

Implication for the CTX infection host specificity

— In this work, we observed that the CTX phage protein pIII-N1 responsible for host selection (5) can bind the TolAIII receptor domain from at least three other vibrio species: *V. alginolyticus*, *V. anguillarum* and *V. tasmaniensis* (Fig. 7).

However, the host range reported for CTX from environmental sampling studies is surprisingly narrow, even in species carrying a conserved TolA sequence. Thus, while all the epidemic *V. cholerae* strains belonging to the O1 or O139 serogroups carry the CTX prophage, it is rarely detected (2 to 5 %) in non-O1/non-O139 *V. cholerae* environmental isolate genomes (55–59). Apart from *Vibrio cholerae*, CTX Φ has been reported to infrequently infect other *Vibrio* species, even for very close species such as *V. mimicus* (60). It has been proposed that the limited distribution of the primary receptor TCP among vibrio species plays a predominant role in the fate of the entire infection process (55). It is interesting to note that TCP-independent CTX Φ infection has been reported to occur in defined conditions (5). Thus, while TolA is a conserved protein, variation in the sequence of the TolAIII domain might serve as a second level of CTX Φ host specificity checkpoint.

Since bacteriophages, like any other viruses are obligate intracellular parasites, successful uptake across the bacterial cell envelope is an essential condition to complete their life cycle. However, current knowledge on host-phage interactions is based on a limited number of microbial models. This scientific problem outreaches the question of *V. cholerae* pathogenic conversion, as other filamentous phages (sharing similarities with CTX Φ) have been demonstrated to affect the virulence and fitness of a large range of bacterial host: MDA in invasive isolates of *Neisseria meningitides* (61), Ypf Φ in the plague bacillus, *Yersinia pestis* (62), CUS-1 in the high-virulence clone *Escherichia coli* O18:K1:H7 (63). In this context, our work emphasizes the necessity to study CTX Φ infection on its own, and to overtake the Ff coliphage model of infection. It also sheds light on the mechanism underlying the initial filamentous phage –bacterial host binding, and provides basic knowledge that might serve the understanding of transduction-dependent spreading of virulence factors in bacterial populations.

Experimental Procedures

Bacterial strains and growth conditions— Relevant bacterial strains and plasmids used in this study are listed in Table S1. Bacteria were routinely cultivated in Luria-Bertani broth (LB,

407 mOsM) at 37°C (*E. coli*) or 30°C (*V. cholerae*). When specified, MgCl₂ (2 mM) was added to the culture medium to promote OM integrity and cell growth of *tol* mutants. Tryptone broth (1% (w/v) Tryptone, 66 mM NaCl; pH 8.5) was used as a low osmolarity medium (123 mOsM, (64)). When indicated, antibiotics were added to the medium at the following concentrations: streptomycin (100 µg/ml), ampicillin (50 or 100 µg/ml), kanamycin (50 µg/ml), chloramphenicol (30 µg/ml for *E. coli*, 1 µg/ml for *V. cholerae*). *V. cholerae tolA* Δ(41-421) in frame deletion mutant was constructed as previously described using the primers listed in Table S2 and the suicide plasmid pWM91 (65, 66). The absence of the TolA protein in the mutant strain was confirmed by western blotting using polyclonal antibodies directed against *E. coli* TolAII-III protein (30) and cross-reacting with TolAIII^{Vc}.

Plasmid construction. Polymerase Chain Reactions (PCR) were performed using Q5 High Fidelity DNA polymerase (NewEngland Biolabs). Primer sets required to generate genetic constructs were synthesized by Sigma Aldrich (Table S2). Enzymes (NewEngland Biolabs) were used according to the manufacturer's instructions. Plasmids have been constructed either by standard restriction/ligation protocol, by Sequence and Ligase Independent Cloning (SLIC) (67) as modified by Jeong and collaborators (68), or by Restriction-Free (RF) cloning as previously described (69). Briefly for RF cloning, genes of interest were amplified with oligonucleotides introducing extensions annealing to the target vector. The double-stranded product of the first PCR has then been used as oligonucleotides for a second PCR using the target vector as template and Pfu Turbo polymerase (Stratagen, La Jolla, CA). For BACTH plasmid constructs, the *V. cholerae* El Tor N16961 genome was used as a template to PCR-amplify the pIII^{CTX} encoding gene (*orfU*, at loci vc1460). The *tolA* sequence was amplified from *V. cholerae* O395 (locus VC0395_A1430) or from *E. coli* W3110 (locus BL257_RS03625) genomes. The pG3 vector (10) was used as a template to amplify pIII^{M13}. Amplified products were cloned into a pUT18c or a pKT25 expression vector (29) to generate fusions with the adenylate cyclase T18 and T25 domains. For construction of the pBAD-TolA rescue plasmid, the native sequence of *V. cholerae*

O395 TolA, retaining the start and the stop codons was amplified by PCR. The forward primer was designed to introduce a Shine Dalgarno consensus sequence GAAGGAGATATACATACCC directly upstream of the start codon. The amplification product was then introduced into the pBAD18-Kan vector (70). For periplasmic expression, pIN-pIII-N1^{CTX} plasmid was constructed by PCR-amplifying the pIII-N1^{CTX} sequence (without start codon) with an upstream oligonucleotide encoding Strep-tag II (WSHPQFEK) and a downstream oligonucleotide encoding a C-terminal 6-His sequence. Digestion of the PCR product and the pIN-ompA2 vector (33) with EcoRI and BamHI enzymes allowed subsequent ligation of the PCR product into the vector. The pIN-pIII-N1^{M13} plasmid (previously named pG3) has been previously described (10).

Mutations on pUT18-TolA, pKT25-pIII-N1, pIN-pIII-N1 and pBAD-TolA plasmids were performed by Quick-change site-directed mutagenesis using complementary pairs of oligonucleotides (listed in Table S2) and Pfu Turbo polymerase. All constructs were confirmed by DNA sequencing (Eurofins, MWG).

Construction of the Oxi-BTH strain—In order to conduct bacterial two-hybrid experiments in an oxidative environment, the *E. coli* K12 SHuffle T7 strain (New England Biolabs) was engineered further. This initial strain is deleted for glutaredoxin reductase (*gor*) and thioredoxin reductase (*trxB*) genes, which allows disulfide bonds formation in the cytoplasm. Moreover, cytoplasmic expression of the disulfide bond isomerase DsbC acts on proteins with multiple disulfide bonds, promoting correct disulfide bond formation and proper folding. In this genetic background, the *cya*^o mutation was transduced using a P1-lysate of an *E. coli* K12 *cya*^o strain. The resulting mutant strain, names Oxi-BTH, was unable to ferment sugars, and consequently grew as white colonies when plated on MacConkey plates.

Bacterial Two-Hybrid Assay in *E. coli* BTH101 and Oxi-BTH strains—The adenylate cyclase-based bacterial two-hybrid technique was used as previously published (29), with the following modifications. Pairs of proteins to be tested were fused to the isolated T18 and T25 catalytic domains of the *Bordetella* adenylate cyclase. After transformation of the two plasmids producing the fusion proteins into the reporter BTH101 or Oxi-

BTH strains, plates were incubated at 37°C for 24 hours. Three colonies for each transformation were inoculated into 600 µl of LB medium supplemented with ampicillin, kanamycin and IPTG (0.5 mM). After overnight growth at 30°C, 5 µl of each culture were dropped onto MacConkey plates supplemented with ampicillin, kanamycin and IPTG (0.5 mM). Plates were incubated for 16 to 24 hrs (BTH101) and 2 to 3 days (Oxi-BTH) at 30°C. The experiments were done at least in triplicate and a representative assay is shown.

SDS-PAGE and Immunoblotting— Protein samples resuspended in 2x loading buffer were subjected to sodium dodecyl sulphate (SDS)-polyacrylamide gel electrophoresis (PAGE). When specified, 2-mercaptoethanol (5% final) was added to the samples. For detection by immunostaining, proteins were transferred onto nitrocellulose membranes, and immunoblots were probed with primary antibodies, and goat secondary antibodies coupled to alkaline phosphatase, and developed in alkaline buffer in presence of 5-bromo-4-chloro-3-indolylphosphate (BCIP) and nitroblue tetrazolium (NBT). The anti-TolAIII^{Ec} polyclonal antibodies is from our laboratory collection while the anti-5 His monoclonal antibody (QIAGEN), the anti-CyaA monoclonal antibody (3D1, Santa Cruz Biotechnology) and alkaline phosphatase-conjugated goat anti-rabbit and anti-mouse antibodies (Millipore) have been purchased as indicated.

V. cholerae phenotypic analysis—

Sensitivity test to SDS. *V. cholerae* cells harboring the empty plasmid as a control, or the plasmid encoding the constructs of interest were grown in LB medium at 30°C until stationary phase, then back diluted to initial OD_{595nm}=0.2 in LB supplemented or not with SDS 0.125%, and grown for 7 hrs at 30°C with agitation. The percentage of surviving cells was estimated from the turbidity ratio of the SDS-treated cells and the control samples. Experiments were performed in triplicates. **Sensitivity test to deoxycholate.** Normalized serial dilutions of strains to be tested were spotted onto 1% deoxycholate (DOC)-supplemented LB plates. After O/N incubation at 37°C, survival was reported as the highest dilution of strain able to form colonies. **Growth in low osmolarity conditions.** The different strains were grown in LB medium at 30°C until stationary phase, then back diluted 100-fold in LB medium (osmolarity 407 mOsM) and in Tryptone broth

(1% (w/v) Tryptone, 66 mM NaCl; pH 8.5; 123 mOsM, (64)), and incubated for 16 hrs at 30°C. The percentage of growth was estimated from the turbidity ratio of the tested strains and the control sample. Experiments were performed in triplicates.

CTX-cm phage particle preparation— The *difI*⁺ strain BS2 (71) harboring the chloramphenicol-marked CTX^{El Tor} phage replicative form (pCTX-cm) was used as a donor strain to produce CTX phage particles. The donor strain was streaked onto LB cm1 plates, and incubated at 37°C overnight. A single colony was used to inoculate a 2 mL LB + Sm100 culture and incubated at 37°C for 16 hours. Cell were pelleted by centrifugation and the supernatant containing phages was filter-sterilized using 0.22 µm syringe filter. Phage preparation was checked for sterility by plating on LB plate.

Susceptibility to CTX phage infection assays— Cell susceptibility to phage infection was conducted as previously described (72). Briefly, for each recipient strain, 3 independent clones were cultivated separately in TCP-inducing conditions (LB 1% tryptone, 0.5% yeast extract, 0.5% NaCl, pH 6.5, 30°C). After 20 hrs of growth, 75 µl of cells were mixed with 75 µl of CTX-cm phage suspension. The mixture was incubated during 30 min at room temperature without shaking, then 500 µl of LB were added and the cell suspension was incubated at 37°C with vigorous shaking for 45 min to allow cell recovery. Then dilutions of the cell suspension were plated on LB agar plates supplemented with Sm (100) or with Sm (50) Cm (1) to enumerate total cells and transductant cells, respectively. The frequency of infection was determined by dividing the number of transductants by the number of total recipient cells.

NMR spectroscopy— For NMR studies a TolA₂₃₇₋₃₅₆^{Vc} (TolAIII^{Vc}) construct was included in a plasmid with the gene of OmpA signal sequence for protein secretion at the N-terminus and 6-HisTag for the purification at the C-terminus. For the native and variant pIII-N1^{CTX}, OmpA signal sequence and 6-HisTag construct were used, with an additional strepTag at the N-terminal of the gene sequence. ¹⁵N-isotopic labelling of native and mutant pIII-N1^{CTX} were obtained from bacteria grown on M9 medium containing 1g/L ¹⁵NH₄Cl as sole source of nitrogen. The proteins were overexpressed in *E. coli* BL21 strain. Protein

production was obtained after 2h IPTG induction at 37°C. Protein purification was obtained from periplasmic extract pulled on Ni-NTA agarose and eluted with imidazole step gradient.

NMR spectra were recorded on a Bruker 600MHz spectrometer equipped with a TCI cryoprobe, at 300K. ¹H-¹⁵N HSQC spectra were processed with TopSpin software. For NMR experiments pIII-N1^{CTX} wild type and (E37Q-D39N) double mutant, the concentration was 0.16mM in 50mM NaPO₄, 50 mM NaCl buffer at pH 6.9. In the case of the complexes, the final TolAIII^{Vc} concentration was 0.32mM.

In silico analysis — Search for *V. cholerae* O395 TolA orthologous sequences was performed with BlastP, and restricted to Vibrionaceae species using TaxReport (<http://annotathon.org/>). Multisequence alignments were performed using Clustal Omega (73) and color coded with JalView2 tool (74). The 2P2I database (51, 52) was used to list all the non-bonded contacts at the complex interface (PDB #4G7X) with a cut-off distance of 4 Å.

Acknowledgements— We thank François-Xavier Barre, Paula Watnick, Delphine Destoumieux-gazon, Marie-Stephanie Aschteng, Long-Fei Wu and Emmanuelle Bouveret for providing useful strains and plasmids. We thank Emmanuelle Bouveret, Eric Cascales, Bérengère Ize, Marlon Sidore and all the members of the LISM for helpful

discussion and support, Annick Brun, Isabelle Bringer, Moly Ba, Olivier Uderso and Faniry Raboanarivola for technical assistance and Octave Uhleure for encouragements. The authors thank Olivier Bornet at the NMR platform of IMM for NMR time machine necessary for recording NMR spectra. Work in R.L. and F.G. laboratory is supported by the Centre National de la Recherche Scientifique (CNRS) and the Aix-Marseille Univ. R.L. research team benefits grants from Agence Nationale de la Recherche (ANR-14-CE09-0023). L.H. was supported by a postdoctoral fellowship from Fondation pour la Recherche Médicale (FRM, SPF20100518724), and R.N. is supported by a Ph.D fellowship from the French Ministry of Research.

Conflict of interest—The authors declare that they have no conflicts of interest with the contents of this article.

Author contributions— LH, MN, FG, DD and RL contributed to the design of the study; LH, RN, MN and FG performed experiments. LH, RN, MN, FG, DD and RL contributed to data interpretation. LH wrote most of the manuscript. All authors approved the final version of the manuscript.

References

1. Waldor, M. K., and Mekalanos, J. J. (1996) Lysogenic conversion by a filamentous phage encoding cholera toxin. *Science*. **272**, 1910–1914
2. Mai-Prochnow, A., Hui, J. G. K., Kjelleberg, S., Rakonjac, J., McDougald, D., and Rice, S. A. (2015) “Big things in small packages: the genetics of filamentous phage and effects on fitness of their host.” *FEMS Microbiology Reviews*. **39**, 465–487
3. Rakonjac, J., Bennett, N. J., Spagnuolo, J., Gagic, D., and Russel, M. (2011) Filamentous bacteriophage: biology, phage display and nanotechnology applications. *Current issues in molecular biology*. **13**, 51
4. Holliger, P., and Riechmann, L. (1997) A conserved infection pathway for filamentous bacteriophages is suggested by the structure of the membrane penetration domain of the minor coat protein g3p from phage fd. *Structure*. **5**, 265–275
5. Heilpern, A. J., and Waldor, M. K. (2003) pIIICTX, a Predicted CTX Minor Coat Protein, Can Expand the Host Range of Coliphage fd To Include *Vibrio cholerae*. *Journal of Bacteriology*. **185**, 1037–1044
6. Heilpern, A. J., and Waldor, M. K. (2000) CTXφ infection of *Vibrio cholerae* requires the tolQRA gene products. *Journal of bacteriology*. **182**, 1739–1747
7. Deng, L.-W., and Perham, R. N. (2002) Delineating the Site of Interaction on the pIII Protein of

- Filamentous Bacteriophage fd with the F-pilus of Escherichia coli. *Journal of Molecular Biology*. **319**, 603–614
8. Lubkowski, J., Hennecke, F., Plückthun, A., and Wlodawer, A. (1999) Filamentous phage infection: crystal structure of g3p in complex with its coreceptor, the C-terminal domain of TolA. *Structure*. **7**, 711–722
 9. Lubkowski, J., Hennecke, F., Plückthun, A., and Wlodawer, A. (1998) The structural basis of phage display elucidated by the crystal structure of the N-terminal domains of g3p. *Nature Structural Biology*. **5**, 140–147
 10. Pommier, S., Gavioli, M., Cascales, E., and Lloubes, R. (2005) Tol-Dependent Macromolecule Import through the Escherichia coli Cell Envelope Requires the Presence of an Exposed TolA Binding Motif. *Journal of Bacteriology*. **187**, 7526–7534
 11. Riechmann, L., and Holliger, P. (1997) The C-terminal domain of TolA is the coreceptor for filamentous phage infection of E. coli. *Cell*. **90**, 351–360
 12. Deprez, C., Lloubès, R., Gavioli, M., Marion, D., Guerlesquin, F., and Blanchard, L. (2005) Solution Structure of the E.coli TolA C-terminal Domain Reveals Conformational Changes upon Binding to the Phage g3p N-terminal Domain. *Journal of Molecular Biology*. **346**, 1047–1057
 13. Bennett, N. J., and Rakonjac, J. (2006) Unlocking of the Filamentous Bacteriophage Virion During Infection is Mediated by the C Domain of pIII. *Journal of Molecular Biology*. **356**, 266–273
 14. Ng, D., Harn, T., Altindal, T., Kolappan, S., Marles, J. M., Lala, R., Spielman, I., Gao, Y., Hauke, C. A., Kovacikova, G., and others (2016) The Vibrio cholerae Minor Pilin TcpB Initiates Assembly and Retraction of the Toxin-Coregulated Pilus. *PLoS pathogens*. **12**, e1006109
 15. Ford, C. G., Kolappan, S., Phan, H. T. H., Waldor, M. K., Winther-Larsen, H. C., and Craig, L. (2012) Crystal Structures of a CTX pIII Domain Unbound and in Complex with a Vibrio cholerae TolA Domain Reveal Novel Interaction Interfaces. *Journal of Biological Chemistry*. **287**, 36258–36272
 16. Lloubès, R., Cascales, E., Walburger, A., Bouveret, E., Lazdunski, C., Bernadac, A., and Journet, L. (2001) The Tol-Pal proteins of the Escherichia coli cell envelope: an energized system required for outer membrane integrity? *Research in Microbiology*. **152**, 523–529
 17. Sturgis, J. N. (2001) Organisation and evolution of the tol-pal gene cluster. *J Mol Microbiol Biotechnol*. **3**, 113–22
 18. Gray, A. N., Egan, A. J., Van't Veer, I. L., Verheul, J., Colavin, A., Koumoutsis, A., Biboy, J., Altelaar, A. M., Damen, M. J., Huang, K. C., and others (2015) Coordination of peptidoglycan synthesis and outer membrane constriction during Escherichia coli cell division. *Elife*. **4**, e07118
 19. Gully, D., and Bouveret, E. (2006) A protein network for phospholipid synthesis uncovered by a variant of the tandem affinity purification method in Escherichia coli. *PROTEOMICS*. **6**, 282–293
 20. Cascales, E., Gavioli, M., Sturgis, J. N., and Lloubès, R. (2000) Proton motive force drives the interaction of the inner membrane TolA and outer membrane pal proteins in Escherichia coli. *Mol. Microbiol.* **38**, 904–915
 21. Cascales, E., Lloubes, R., and Sturgis, J. N. (2001) The TolQ–TolR proteins energize TolA and share homologies with the flagellar motor proteins MotA–MotB. *Molecular microbiology*. **42**, 795–807
 22. Walburger, A., Lazdunski, C., and Corda, Y. (2002) The Tol/Pal system function requires an interaction between the C-terminal domain of TolA and the N-terminal domain of TolB. *Molecular microbiology*. **44**, 695–708
 23. Cascales, E., and Lloubès, R. (2003) Deletion analyses of the peptidoglycan-associated lipoprotein Pal reveals three independent binding sequences including a TolA box: Pal interacts independently with OmpA, TolA and TolB. *Molecular Microbiology*. **51**, 873–885
 24. Lloubès, R., Cascales, E., Walburger, A., Bouveret, E., Lazdunski, C., Bernadac, A., and Journet, L. (2001) The Tol-Pal proteins of the Escherichia coli cell envelope: an energized system required for outer membrane integrity? *Res. Microbiol.* **152**, 523–529
 25. Gerding, M. A., Ogata, Y., Pecora, N. D., Niki, H., and de Boer, P. A. J. (2007) The trans - envelope Tol-Pal complex is part of the cell division machinery and required for proper outer-

- membrane invagination during cell constriction in *E. coli*. *Molecular Microbiology*. **63**, 1008–1025
26. Yeh, Y.-C., Comolli, L. R., Downing, K. H., Shapiro, L., and McAdams, H. H. (2010) The Caulobacter Tol-Pal Complex Is Essential for Outer Membrane Integrity and the Positioning of a Polar Localization Factor. *Journal of Bacteriology*. **192**, 4847–4858
 27. Santos, T. M. A., Lin, T.-Y., Rajendran, M., Anderson, S. M., and Weibel, D. B. (2014) Polar localization of *Escherichia coli* chemoreceptors requires an intact Tol-Pal complex: Chemoreceptor localization in *Escherichia coli*. *Molecular Microbiology*. **92**, 985–1004
 28. Li, C., Zhang, Y., Vankemmelbeke, M., Hecht, O., Aleanizy, F. S., Macdonald, C., Moore, G. R., James, R., and Penfold, C. N. (2012) Structural Evidence That Colicin A Protein Binds to a Novel Binding Site of TolA Protein in *Escherichia coli* Periplasm. *Journal of Biological Chemistry*. **287**, 19048–19057
 29. Karimova, G., Pidoux, J., Ullmann, A., and Ladant, D. (1998) A bacterial two-hybrid system based on a reconstituted signal transduction pathway. *Proc. Natl. Acad. Sci. U.S.A.* **95**, 5752–5756
 30. Derouiche, R., Zeder-Lutz, G., Bénédicti, H., Gavioli, M., Rigal, A., Lazdunski, C., and Lloubès, R. (1997) Binding of colicins A and E1 to purified TolA domains. *Microbiology (Reading, Engl.)*. **143** (Pt 10), 3185–3192
 31. Lobstein, J., Emrich, C. A., Jeans, C., Faulkner, M., Riggs, P., and Berkmen, M. (2012) SHuffle, a novel *Escherichia coli* protein expression strain capable of correctly folding disulfide bonded proteins in its cytoplasm. *Microb. Cell Fact.* **11**, 56
 32. Martin, A., and Schmid, F. X. (2003) The folding mechanism of a two-domain protein: folding kinetics and domain docking of the gene-3 protein of phage fd. *J. Mol. Biol.* **329**, 599–610
 33. Ghrayeb, J., Kimura, H., Takahara, M., Hsiung, H., Masui, Y., and Inouye, M. (1984) Secretion cloning vectors in *Escherichia coli*. *EMBO J.* **3**, 2437–2442
 34. Bouveret, E., Rigal, A., Lazdunski, C., and Bénédicti, H. (1998) Distinct regions of the colicin A translocation domain are involved in the interaction with TolA and TolB proteins upon import into *Escherichia coli*. *Mol. Microbiol.* **27**, 143–157
 35. Meury, J., and Devilliers, G. (1999) Impairment of cell division in tolA mutants of *Escherichia coli* at low and high medium osmolarities. *Biol. Cell.* **91**, 67–75
 36. Levensgood, S. K., Beyer, W. F., and Webster, R. E. (1991) TolA: a membrane protein involved in colicin uptake contains an extended helical region. *Proc. Natl. Acad. Sci. U.S.A.* **88**, 5939–5943
 37. Buchan, D. W. A., Minneci, F., Nugent, T. C. O., Bryson, K., and Jones, D. T. (2013) Scalable web services for the PSIPRED Protein Analysis Workbench. *Nucleic Acids Res.* **41**, W349–357
 38. Tomasi, M., Battistini, A., Araco, A., Roda, L. G., and D’Agno, G. (1979) The role of the reactive disulfide bond in the interaction of cholera-toxin functional regions. *Eur. J. Biochem.* **93**, 621–627
 39. Craig, L., Pique, M. E., and Tainer, J. A. (2004) Type IV pilus structure and bacterial pathogenicity. *Nat. Rev. Microbiol.* **2**, 363–378
 40. Gao, Y., Hauke, C. A., Marles, J. M., and Taylor, R. K. (2016) Effects of tcpB Mutations on Biogenesis and Function of the Toxin-Coregulated Pilus, the Type IVb Pilus of *Vibrio cholerae*. *J. Bacteriol.* **198**, 2818–2828
 41. Yang, M., Liu, Z., Hughes, C., Stern, A. M., Wang, H., Zhong, Z., Kan, B., Fenical, W., and Zhu, J. (2013) Bile salt-induced intermolecular disulfide bond formation activates *Vibrio cholerae* virulence. *Proc. Natl. Acad. Sci. U.S.A.* **110**, 2348–2353
 42. Morgan, S. J., French, E. L., Thomson, J. J., Seaborn, C. P., Shively, C. A., and Krukons, E. S. (2015) Formation of an Intramolecular Periplasmic Disulfide Bond in TcpP Protects TcpP and TcpH from Degradation in *Vibrio cholerae*. *J. Bacteriol.* **198**, 498–509
 43. Fengler, V. H. I., Boritsch, E. C., Tutz, S., Seper, A., Ebner, H., Roier, S., Schild, S., and Reidl, J. (2012) Disulfide Bond Formation and ToxR Activity in *Vibrio cholerae*. *PLoS ONE*. **7**, e47756
 44. Battesti, A., and Bouveret, E. (2012) The bacterial two-hybrid system based on adenylate cyclase reconstitution in *Escherichia coli*. *Methods*. **58**, 325–334
 45. Ouellette, S. P., Gauliard, E., Antosová, Z., and Ladant, D. (2014) A Gateway®-compatible bacterial adenylate cyclase-based two-hybrid system. *Environ Microbiol Rep.* **6**, 259–267

46. Handford, J. I., Ize, B., Buchanan, G., Butland, G. P., Greenblatt, J., Emili, A., and Palmer, T. (2009) Conserved Network of Proteins Essential for Bacterial Viability. *Journal of Bacteriology*. **191**, 4732–4749
47. Houot, L., Fanni, A., de Bentzmann, S., and Bordi, C. (2012) A bacterial two-hybrid genome fragment library for deciphering regulatory networks of the opportunistic pathogen *Pseudomonas aeruginosa*. *Microbiology*. **158**, 1964–1971
48. Gaspar, J. A., Thomas, J. A., Marolda, C. L., and Valvano, M. A. (2000) Surface expression of O-specific lipopolysaccharide in *Escherichia coli* requires the function of the TolA protein. *Mol. Microbiol.* **38**, 262–275
49. Dennis, J. J., Lafontaine, E. R., and Sokol, P. A. (1996) Identification and characterization of the tolQRA genes of *Pseudomonas aeruginosa*. *J. Bacteriol.* **178**, 7059–7068
50. Lorenz, S. H., Jakob, R. P., Weininger, U., Balbach, J., Dobbek, H., and Schmid, F. X. (2011) The filamentous phages fd and IF1 use different mechanisms to infect *Escherichia coli*. *J. Mol. Biol.* **405**, 989–1003
51. Basse, M. J., Betzi, S., Bourgeas, R., Bouzidi, S., Chetrit, B., Hamon, V., Morelli, X., and Roche, P. (2013) 2P2Idb: a structural database dedicated to orthosteric modulation of protein-protein interactions. *Nucleic Acids Res.* **41**, D824–827
52. Basse, M.-J., Betzi, S., Morelli, X., and Roche, P. (2016) 2P2Idb v2: update of a structural database dedicated to orthosteric modulation of protein-protein interactions. *Database (Oxford)*. 10.1093/database/baw007
53. Bonsor, D. A., Hecht, O., Vankemmelbeke, M., Sharma, A., Krachler, A. M., Housden, N. G., Lilly, K. J., James, R., Moore, G. R., and Kleanthous, C. (2009) Allosteric beta-propeller signalling in TolB and its manipulation by translocating colicins. *EMBO J.* **28**, 2846–2857
54. Sinha, N., and Smith-Gill, S. J. (2002) Electrostatics in protein binding and function. *Curr. Protein Pept. Sci.* **3**, 601–614
55. Faruque, S. M., Asadulghani, null, Saha, M. N., Alim, A. R., Albert, M. J., Islam, K. M., and Mekalanos, J. J. (1998) Analysis of clinical and environmental strains of nontoxigenic *Vibrio cholerae* for susceptibility to CTXPhi: molecular basis for origination of new strains with epidemic potential. *Infect. Immun.* **66**, 5819–5825
56. Hasan, N. A., Ceccarelli, D., Grim, C. J., Taviani, E., Choi, J., Sadique, A., Alam, M., Siddique, A. K., Sack, R. B., Huq, A., and Colwell, R. R. (2013) Distribution of virulence genes in clinical and environmental *Vibrio cholerae* strains in Bangladesh. *Appl. Environ. Microbiol.* **79**, 5782–5785
57. Ceccarelli, D., Chen, A., Hasan, N. A., Rashed, S. M., Huq, A., and Colwell, R. R. (2015) Non-O1/non-O139 *Vibrio cholerae* carrying multiple virulence factors and *V. cholerae* O1 in the Chesapeake Bay, Maryland. *Appl. Environ. Microbiol.* **81**, 1909–1918
58. Jiang, S., Chu, W., and Fu, W. (2003) Prevalence of cholera toxin genes (ctxA and zot) among non-O1/O139 *Vibrio cholerae* strains from Newport Bay, California. *Appl. Environ. Microbiol.* **69**, 7541–7544
59. Sarkar, A., Nandy, R. K., Nair, G. B., and Ghose, A. C. (2002) *Vibrio* pathogenicity island and cholera toxin genetic element-associated virulence genes and their expression in non-O1 non-O139 strains of *Vibrio cholerae*. *Infect. Immun.* **70**, 4735–4742
60. Boyd, E. F., Moyer, K. E., Shi, L., and Waldor, M. K. (2000) Infectious CTXPhi and the *vibrio* pathogenicity island prophage in *Vibrio mimicus*: evidence for recent horizontal transfer between *V. mimicus* and *V. cholerae*. *Infect. Immun.* **68**, 1507–1513
61. Bille, E., Zahar, J.-R., Perrin, A., Morelle, S., Kriz, P., Jolley, K. A., Maiden, M. C. J., Dervin, C., Nassif, X., and Tinsley, C. R. (2005) A chromosomally integrated bacteriophage in invasive meningococci. *J. Exp. Med.* **201**, 1905–1913
62. Derbise, A., Chenal-Francisque, V., Pouillot, F., Fayolle, C., Prévost, M.-C., Médigue, C., Hinnebusch, B. J., and Carniel, E. (2007) A horizontally acquired filamentous phage contributes to the pathogenicity of the plague bacillus. *Mol. Microbiol.* **63**, 1145–1157
63. Gonzalez, M. D., Lichtensteiger, C. A., Caughlan, R., and Vimr, E. R. (2002) Conserved filamentous prophage in *Escherichia coli* O18:K1:H7 and *Yersinia pestis* biovar orientalis. *J.*

Bacteriol. **184**, 6050–6055

64. Goforth, J. B., Walter, N. E., and Karatan, E. (2013) Effects of polyamines on *Vibrio cholerae* virulence properties. *PLoS ONE*. **8**, e60765
65. Metcalf, W. W., Jiang, W., Daniels, L. L., Kim, S. K., Haldimann, A., and Wanner, B. L. (1996) Conditionally replicative and conjugative plasmids carrying lacZ alpha for cloning, mutagenesis, and allele replacement in bacteria. *Plasmid*. **35**, 1–13
66. Houot, L., and Watnick, P. I. (2007) A Novel Role for Enzyme I of the *Vibrio cholerae* Phosphoenolpyruvate Phosphotransferase System in Regulation of Growth in a Biofilm. *Journal of Bacteriology*. **190**, 311–320
67. Li, M. Z., and Elledge, S. J. (2007) Harnessing homologous recombination in vitro to generate recombinant DNA via SLIC. *Nat. Methods*. **4**, 251–256
68. Jeong, J.-Y., Yim, H.-S., Ryu, J.-Y., Lee, H. S., Lee, J.-H., Seen, D.-S., and Kang, S. G. (2012) One-step sequence- and ligation-independent cloning as a rapid and versatile cloning method for functional genomics studies. *Appl. Environ. Microbiol.* **78**, 5440–5443
69. van den Ent, F., and Löwe, J. (2006) RF cloning: a restriction-free method for inserting target genes into plasmids. *J. Biochem. Biophys. Methods*. **67**, 67–74
70. Guzman, L.-M., Belin, D., Carson, M. J., and Beckwith, J. O. N. (1995) Tight regulation, modulation, and high-level expression by vectors containing the arabinose PBAD promoter. *Journal of bacteriology*. **177**, 4121–4130
71. Das, B., Bischerour, J., Val, M.-E., and Barre, F.-X. (2010) Molecular keys of the tropism of integration of the cholera toxin phage. *Proc. Natl. Acad. Sci. U.S.A.* **107**, 4377–4382
72. Kirn, T. J., Lafferty, M. J., Sandoe, C. M., and Taylor, R. K. (2000) Delineation of pilin domains required for bacterial association into microcolonies and intestinal colonization by *Vibrio cholerae*. *Molecular microbiology*. **35**, 896–910
73. McWilliam, H., Li, W., Uludag, M., Squizzato, S., Park, Y. M., Buso, N., Cowley, A. P., and Lopez, R. (2013) Analysis Tool Web Services from the EMBL-EBI. *Nucleic Acids Res.* **41**, W597–600
74. Waterhouse, A. M., Procter, J. B., Martin, D. M. A., Clamp, M., and Barton, G. J. (2009) Jalview Version 2--a multiple sequence alignment editor and analysis workbench. *Bioinformatics*. **25**, 1189–1191

FIGURE LEGENDS

FIGURE 1. The pIII-N1^{CTX} and pIII-N1^{M13} domains specifically interact with their cognate TolA partner. (A) Crystal structure of *V. cholerae* TolAIII (yellow) in complex with CTXΦ pIII-N1 (grey, PDB #4G7X), and superimposed to *E. coli* TolAIII (red) in complex with M13Φ pIII-N1 (green, PDB #1TOL). (B) Bacterial two hybrid assay: *E. coli* BTH101 or Oxi-BTH reporter cells producing the indicated domains fused to the T18 or T25 domain of the *Bordetella pertussis* adenylate cyclase were spotted on MacConkey plates. The red color of the spot reflects the interaction between tested domains. ColA^N (N-terminal colicin A domain), pIII-N1^{CTX} (N-ter domain of CTXΦ pIII protein), pIII-N1^{M13} (N-ter domain of M13-phage pIII protein), TolAIII (C-ter domain of *E. coli* or *V. cholerae* TolA protein).

FIGURE 2. pIII-N1^{CTX} disulfide bonds II and III are required for TolAIII^{Vc} interaction. (A) Schematic representation of disulfide bond localization (according to (15)) on the secondary structure of TolAIII^{Vc} and pIII-N1^{CTX}, and (B) representation of disulfide bonds on the crystal structure of the complex. Disulfide bonds in pIII-N1 are numbered I to IV and colored in red. Italic numbers refer to cysteine residue positions. (C) Oxidative bacterial two-hybrid assay : Oxi-BTH reporter cells producing the T25 domain fused to pIII-N1^{CTX}, pIII-N1N2^{CTX} or pIII-N2^{CTX} domains, and the T18 domain fused to *V.*

cholerae TolAIII were spotted on MacConkey plates. Variants bearing substitutions aimed to abolish each of the four disulfide bonds in the pIII-N1^{CTX} domain (C32S, C47S, C75S, C96S) or in TolAIII^{Vc} (C292S) are presented. TolAIII^{Ec} and pIII-N1^{M13} are used as a controls. n.t. not tested.

FIGURE 3. pIII-N1^{CTX}-TolAIII^{Vc} binding relies on two salt bridges. (A) Left: schematic representation of the *V. cholerae* TolAIII and CTX phage pIII-N1 secondary structure. Residues (black arrows) engaged into intermolecular salt-bridges (dotted lines) and disulfide bonds (black lines) are pointed out. Right : x-ray structure of the complex showing the three key salt bridges. (B) Western immunoblot of 0.2 OD units of whole-cell lysates of *E. coli* DH5 α strain carrying T18-TolAIII^{Vc} construct, or variants of interest, and probed with anti-T18 antibody. The molecular weight markers (in kDa) are indicated on the left. (C) TolAIII^{Vc} and pIII-N1^{CTX} point mutants were tested for their binding ability, in comparison to the wild type constructs, in an Oxi-BTH assay on MacConkey plates. TolAIII^{Ec} and pIII-N1^{M13} are used as a controls. n.t. not tested.

FIGURE 4. (A) ¹H-¹⁵N HSQC of ¹⁵N-labelled pIII-N1^{CTX} domain, (B) ¹H-¹⁵N HSQC of ¹⁵N-labelled pIII-N1^{CTX} domain in the absence (in black) and in the presence of TolAIII^{Vc} domain (in red), (C) ¹H-¹⁵N HSQC of ¹⁵N-labelled pIII-N1^{CTX} (E92K) domain, (D) ¹H-¹⁵N HSQC of ¹⁵N-labelled pIIIN1^{CTX} (E92K) domain in the absence (in black) and in the presence of TolAIII^{Vc} domain (in red). (E) ¹H-¹⁵N HSQC of ¹⁵N-labelled pIIIN1^{CTX} (E37Q-D39N) domain, (F) ¹H-¹⁵N HSQC of ¹⁵N-labelled pIIIN1^{CTX} (E37Q-D39N) domain in the absence (in black) and in the presence of TolAIII^{Vc} domain (in red).

FIGURE 5. Periplasmic production of CTX Φ pIII-N1 domain or variants in *V. cholerae* and phenotypic characterization. Precultures of *V. cholerae* O395 cells carrying various pIN constructs were grown in LB supplemented with MgCl₂ to promote OM integrity and cell growth. (A) CTX transduction assay were conducted in triplicate, and CFU were counted on LB or LB supplemented with Cm. Frequency of infection is calculated by dividing the number of transductants (CmR colonies) by the number of O395 recipients. The mean and the standard deviation of the triplicate is presented. For each construct, infection efficiency is expressed as the percentage of infection compared to the receiver strain carrying the empty vector. (B) Membrane integrity assay. 4 μ l of 10-fold dilution of normalized cultures (initial OD₅₉₅=1) were spotted on LB+amp plates alone or supplemented with 1% DOC. (C) Percentage of survival to SDS 0.125% of the different strains compared to *V. cholerae* WT strain carrying a pIN empty vector. For each strain, percentage of growth is calculated as OD_{600 nm} of each stain grown in LB+SDS x 100 / OD_{600 nm} of the WT strain carrying an empty vector and grown in LB. The experiments were conducted in triplicate, and the standard deviation is presented.

FIGURE 6. Phenotypic characterization of *V. cholerae* O395 WT and TolA⁻ strains complemented with TolA variants of interest. (A) Expression of the different pBAD-TolA^{Vc} constructs in *V. cholerae* was assessed by western immunoblotting. A total of 0.3 OD units of whole cell lysate were loaded on a 13.5% acrylamide gel SDS-PAGE and immunodetected using polyclonal antibody raised against *E. coli* TolA. (B) CTX transduction assays were conducted in triplicate, and CFU were counted on LB or LB supplemented with Cm. Frequency of infection is calculated by dividing the number of transductants (CmR colonies) by the number of O395 recipients. The mean and the standard deviation of the triplicate is presented. For each construct, infection efficiency is expressed as the percentage of infection compared to the receiver strain carrying the empty vector. (C) Membrane integrity assay. 4 μ l of 5-fold dilution of normalized cultures (initial OD₆₀₀=1) were spotted on LB+Km plates alone or supplemented with 1% DOC. (D) Percentage of survival to SDS 0.125% of the different strains compared to *V. cholerae* WT strain carrying an pBAD empty vector. For each strain, percentage of growth is calculated as OD_{600 nm} of each stain grown in LB+SDS x 100 / OD_{595 nm} of the WT strain carrying an empty vector and grown in

LB. (E) Quantification of *V. cholerae* O395 WT and TolA- mutant growth in LB (407 mOsm) and in Tryptone broth (TB) supplemented with 66 mM NaCl (123 mOsm). The experiment was conducted in triplicate and the error bars report standard deviations.

FIGURE 7. Conservation of TolA K324 and R325 residues in other *Vibrio* species. (A) Sequence alignment between *V. cholerae*, *V. tasmaniensis*, *V. anguillarum*, *V. alginolyticus*, *V. harveyi* and *V. fisheri* TolAIII β 2- α 2 domain. Residues are colored as follow: basic (black squares), acidic (bold), hydrophobic (light grey), polar uncharged (dark grey). Black arrows point the K324 R325 motif. (B) Western immunoblot of 0.2 OD units of whole-cell lysates of *E. coli* DH5 α strain carrying T18-TolAIII construct from selected Vibrionaceae and from *E. coli*, and probed with anti-Cya antibody. The molecular weight markers (in kDa) are indicated on the left. (C) T18-TolAIII constructs from selected species were tested for their binding ability to the T25-pIII-N1^{CIX} in an Oxi-BTH assay on MacConkey plates. *E. coli* TolAIII and pIII-N1^{M13} are used as a controls. Sequence comparison between each TolAIII of interest and the *V. cholerae* TolAIII amino acid sequences using Blast2 is reported on the right of the panel as E value, identity (I) and positive (P) values.

Figure 1

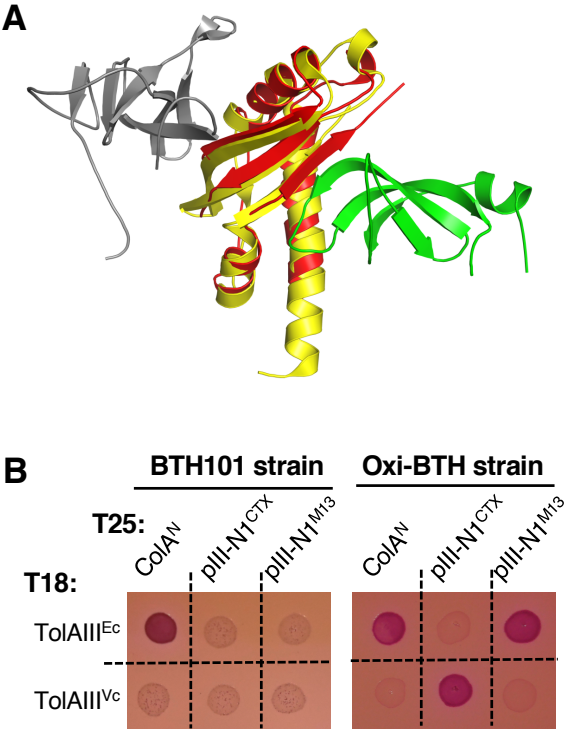


Figure 2

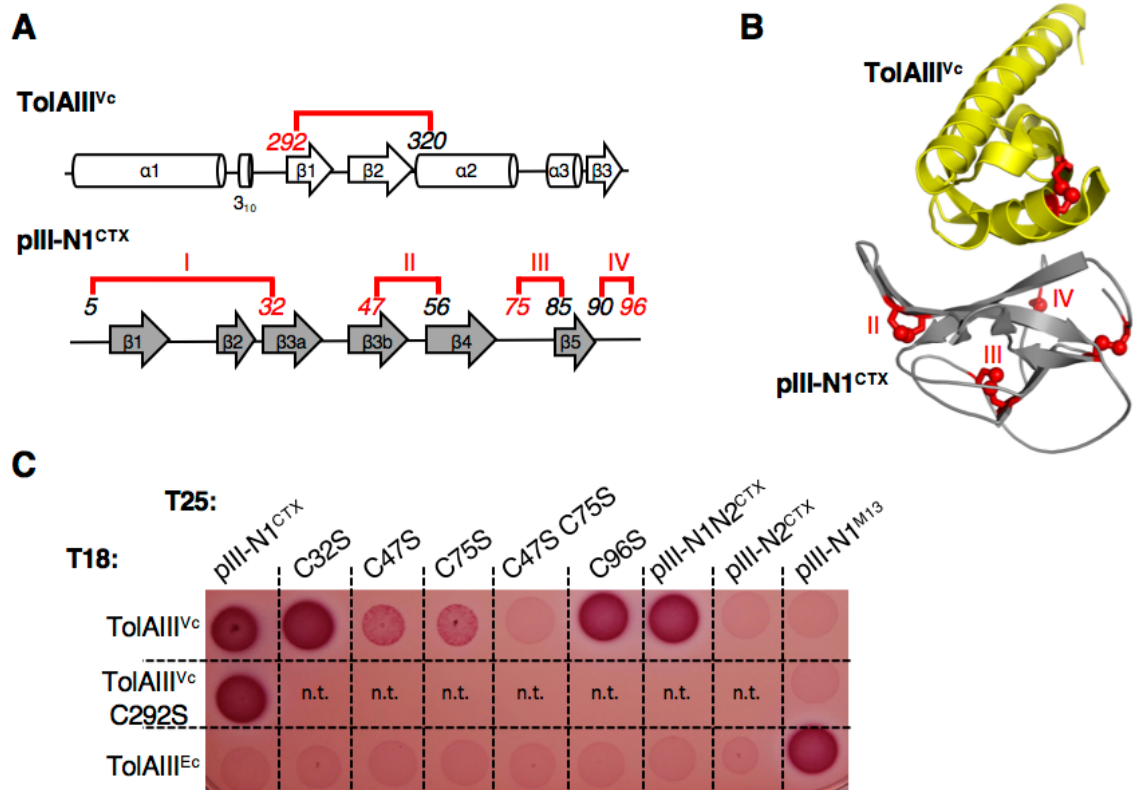


Figure 3

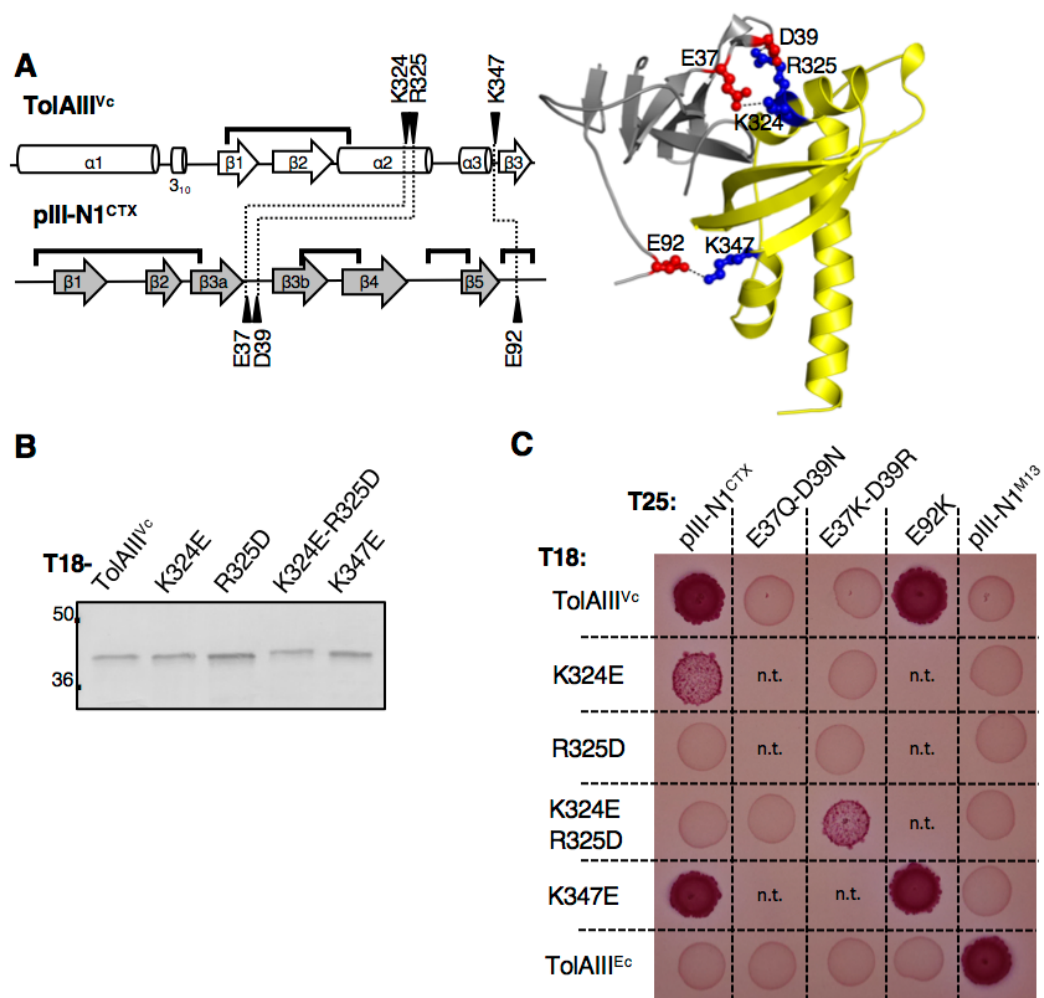


Figure 4

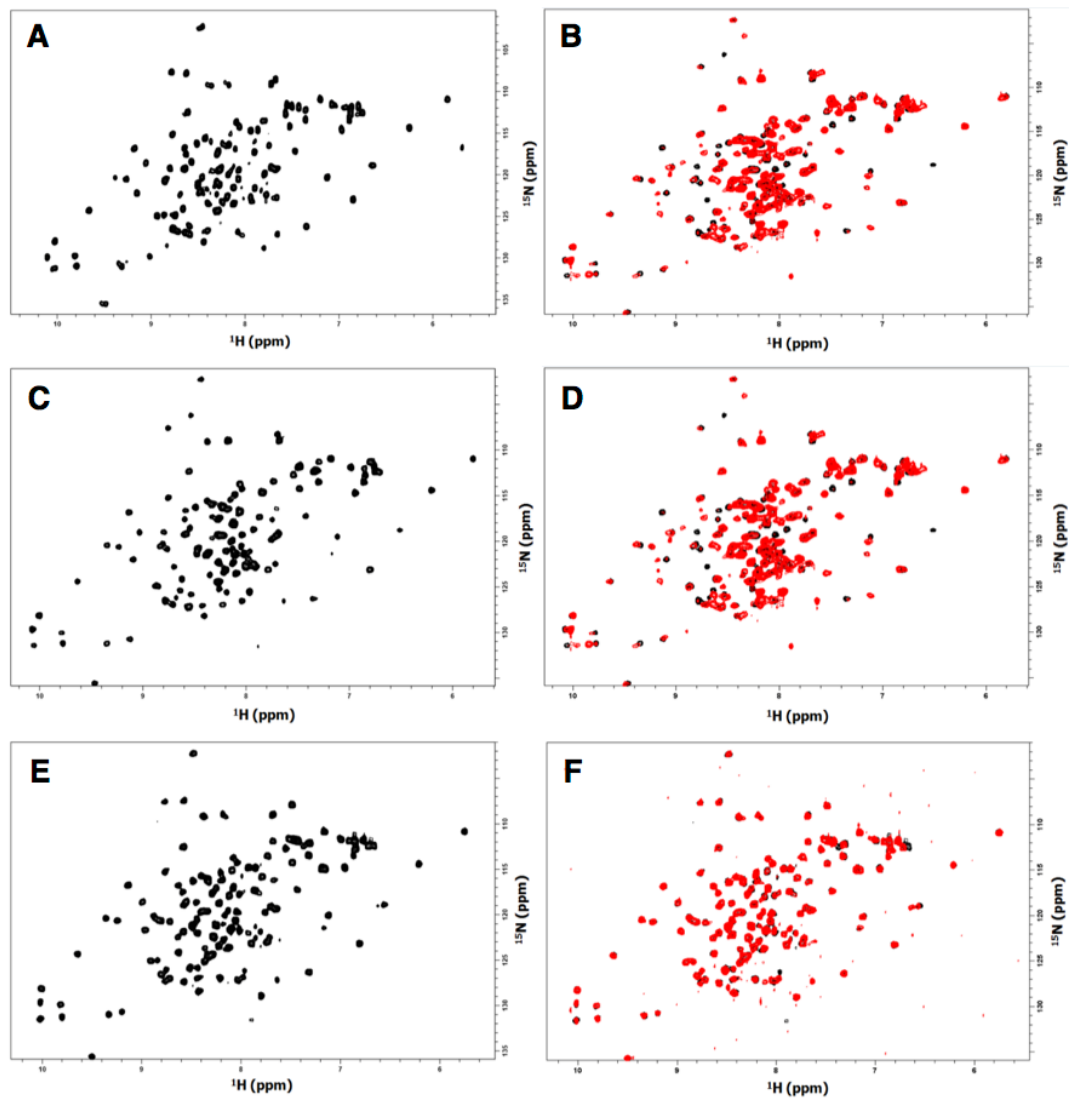
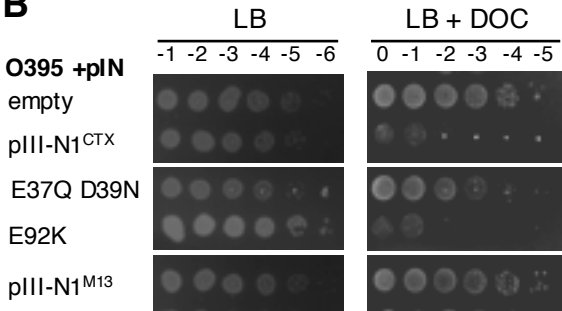


Figure 5

A

O395 + pIN vector	Frequency of infection	SD	Infection efficiency
empty	7.4×10^{-3}	1.1×10^{-3}	100%
CTX pIII-N1	9.8×10^{-4}	2.9×10^{-4}	13%
E37Q D39N	7.9×10^{-3}	6.3×10^{-4}	107%
E92K	1.1×10^{-3}	2.8×10^{-4}	15%
M13 pIII-N1	6.4×10^{-3}	8.3×10^{-4}	87%

B



C

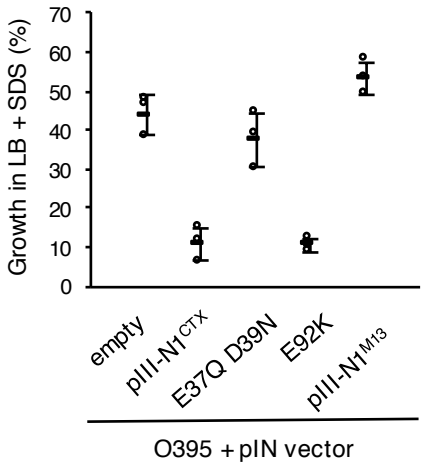
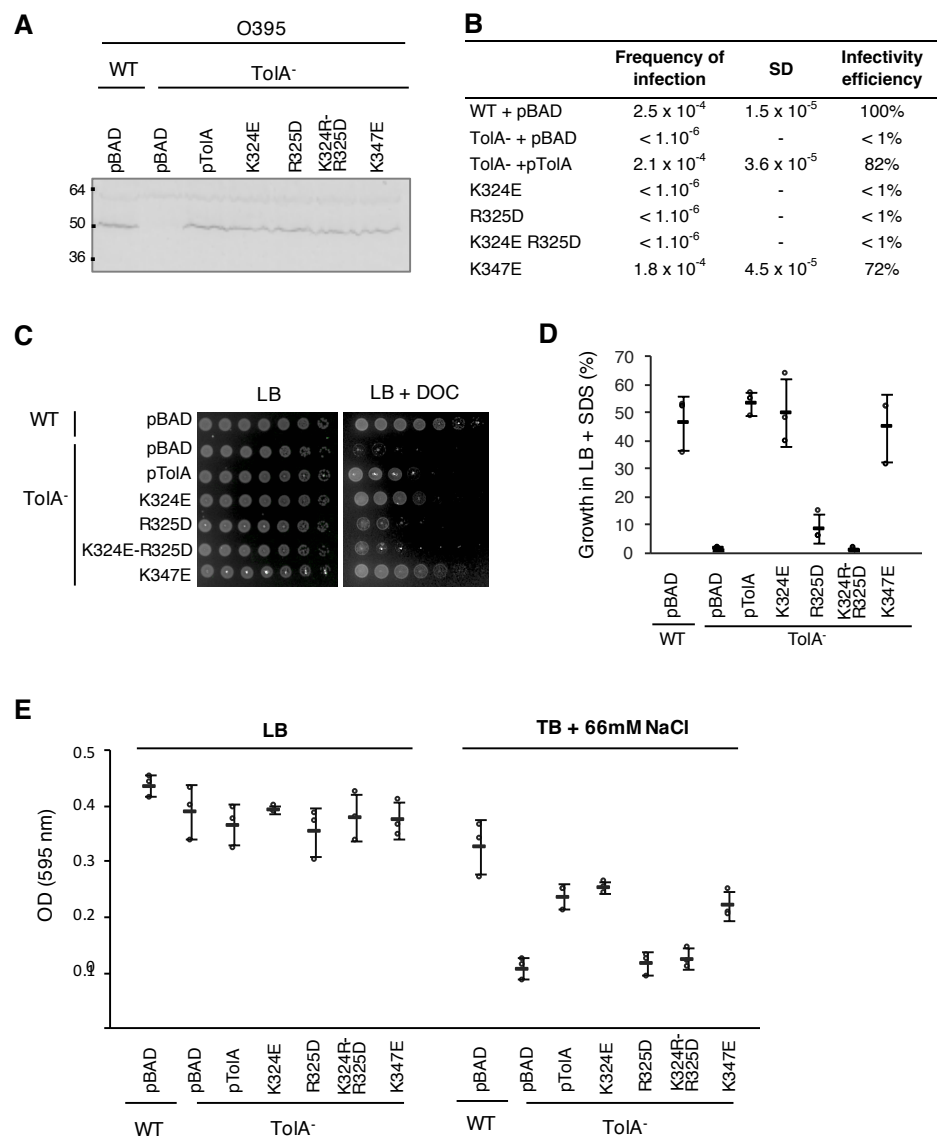
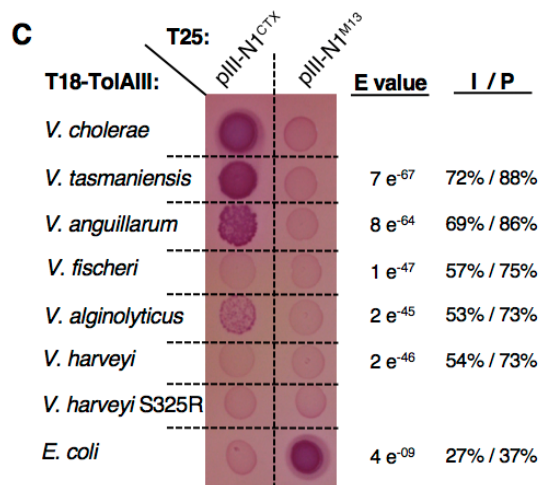
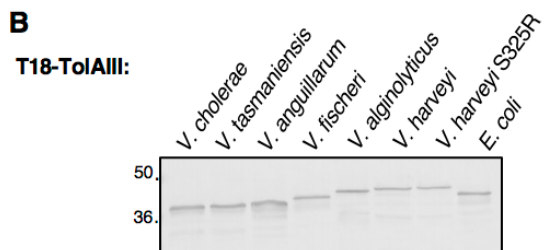
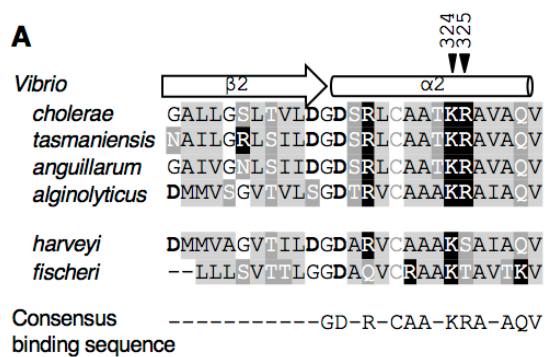


Figure 6



K324E-R325D

Figure 7



Electrostatic interactions between the CTX phage minor coat protein and the bacterial host receptor TolA drives the pathogenic conversion of *Vibrio cholerae*.

Laetitia Houot, Romain Navarro, Matthieu Nouailler, Denis Duché, Françoise Guerlesquin and Roland Lloubes

J. Biol. Chem. published online June 22, 2017

Access the most updated version of this article at doi: [10.1074/jbc.M117.786061](https://doi.org/10.1074/jbc.M117.786061)

Alerts:

- [When this article is cited](#)
- [When a correction for this article is posted](#)

[Click here](#) to choose from all of JBC's e-mail alerts

Supplemental material:

<http://www.jbc.org/content/suppl/2017/06/22/M117.786061.DC1>

This article cites 0 references, 0 of which can be accessed free at

<http://www.jbc.org/content/early/2017/06/22/jbc.M117.786061.full.html#ref-list-1>